



Published in final edited form as:

Toxicol In Vitro. 2007 December ; 21(8) : . doi:10.1016/j.tiv.2007.04.003.

Nanoparticle effects on rat alveolar epithelial cell monolayer barrier properties

Nazanin R. Yacobi^{1,3,*}, Harish C. Phuleria⁴, Lucas Demaio^{1,2}, Chi H. Liang³, Ching-An Peng³, Constantinos Sioutas⁴, Zea Borok^{1,2}, Kwang-Jin Kim^{1,2}, and Edward D. Crandall^{1,2,3}

¹ Will Rogers Institute Pulmonary Research Center, University of Southern California, Los Angeles, CA 90033, USA

² Department of Medicine, University of Southern California, Los Angeles, CA 90033, USA

³ Mork Family Department of Chemical Engineering and Materials Science, University of Southern California, Los Angeles, CA 90033, USA

⁴ Department of Civil and Environmental Engineering, University of Southern California, Los Angeles, CA 90033, USA

Abstract

Inhaled nanoparticles have been reported to contribute to deleterious effects on human health. In this study, we investigated the effects of ultrafine ambient particulate suspensions (UAPS), polystyrene nanoparticles (PNP; positively and negatively charged; 20, 100, 120 nm), quantum dots (QD; positively and negatively charged; 30 nm) and single wall carbon nanotubes (SWCNT) on alveolar epithelial cell barrier properties. Transmonolayer resistance (R_t) and equivalent short-circuit current (I_{eq}) of primary rat alveolar epithelial cell monolayers were measured in the presence and absence of varying concentrations of apical nanoparticles. In some experiments, apical-to-basolateral fluxes of radiolabeled mannitol or inulin were determined with or without apical UAPS exposure and lactate dehydrogenase (LDH) release was analyzed after UAPS or SWCNT exposure. Results revealed that exposure to UAPS decreased R_t and I_{eq} significantly over 24 hours, although neither mannitol nor inulin fluxes changed. Positively charged QD decreased R_t significantly (with subsequent recovery), while negatively charged QD did not. R_t decreased significantly after SWCNT exposure (with subsequent recovery). On the other hand, PNP exposure had no effects on R_t or I_{eq} . No significant increases in LDH release were observed after UAPS or SWCNT exposure. These data indicate that disruption of alveolar epithelial barrier properties due to apical nanoparticle exposure likely involves alteration of cellular transport pathways and is dependent on specific nanoparticle composition, shape and/or surface charge.

Keywords

Lung injury; ultrafine particles; pulmonary toxicity; epithelial transport; primary culture

* To whom correspondence should be addressed: Nazanin R. Yacobi, USC - Keck School of Medicine, 2011 Zonal Avenue, HMR 914, Los Angeles, CA 90033, USA, Office phone: 323 442 1217, Office Fax: 323 442 2611, Email address: nyaghoob@usc.edu.

Publisher's Disclaimer: This is a PDF file of an unedited manuscript that has been accepted for publication. As a service to our customers we are providing this early version of the manuscript. The manuscript will undergo copyediting, typesetting, and review of the resulting proof before it is published in its final citable form. Please note that during the production process errors may be discovered which could affect the content, and all legal disclaimers that apply to the journal pertain.

Introduction

Nanoparticles are commonly defined as particles having at least one dimension of <100 nm. Investigators in environmental health usually refer to particles smaller than 100 nm diameter in ambient air as ultrafine particles. These ultrafine ambient particulates and engineered nanoparticles possess nanostructure-dependent properties due to their small size, chemical composition, surface charge, solubility and/or shape (Oberdorster *et al.* 2005b; Xia *et al.* 2006).

Particulates in ambient air and engineered nanoparticles have increasingly been found to be associated with adverse cardiovascular and pulmonary effects, with suggestions of increased morbidity and mortality in susceptible populations (Oberdorster *et al.* 1995; Oberdorster *et al.* 2005b; Peters *et al.* 2001; Sun *et al.* 2005; Wichmann *et al.* 2000). Since inhaled ambient ultrafine particles can be found in heart, bone marrow, blood vessels and other organs (Nemmar *et al.* 2002; Nemmar *et al.* 2001; Oberdorster 2001), their most likely route of entry into the circulation is across the epithelia of the lung, especially the alveolar epithelium with its very large surface area and thin barrier thickness. Further knowledge about the mechanisms by which particles injure, interact with and/or are transported across the alveolar epithelium is thus of considerable importance for understanding health effects related to inhalation of ultrafine particles in ambient air.

Determination of the characteristics of ambient particulates and engineered nanoparticles that might cause injury, and the mechanisms by which they do so, requires further study (Calcabrini *et al.* 2004; Ghio and Devlin 2001; Oberdorster *et al.* 2005b; Xia *et al.* 2006). Size, shape, charge and/or composition may be important factors that influence how particles affect human health (Alfaro-Moreno *et al.* 2002; Calcabrini *et al.* 2004; Gutierrez-Castillo *et al.* 2006; Oberdorster *et al.* 2005a; Topinka *et al.* 2000; Vedal 1997; Xia *et al.* 2006). Particles smaller than 250 nm are known to reach the distal lung and likely interact with alveolar epithelium. Because of their increased number and surface area as well as their high pulmonary deposition efficiency, ambient ultrafine particles are likely to be important in environmental health (Cassee *et al.* 2002; Donaldson *et al.* 2001; Oberdorster *et al.* 2005b), although some reports have suggested that coarse particles (250 nm < aerodynamic diameter < 10 μm) may be more toxic than fine (aerodynamic diameter < 250 nm) and ultrafine particles (Monn and Becker 1999; Osornio-Vargas *et al.* 2003). Different reports about the consequences of exposure to engineered nanoparticles are inconsistent, with some studies indicating little effect (Geys *et al.* 2006; Muldoon *et al.* 2005; Zhang *et al.* 2006) and others suggesting significant toxicity using both *in vivo* and *in vitro* models (Gurr *et al.* 2005; Magrez *et al.* 2006; Sayes *et al.* 2006; Shvedova *et al.* 2005).

Studies using *in vitro* models have permitted more detailed understanding of important biological properties of the lung *in vivo*, such as the presence of functional epithelial tight junctions and pathways responsible for active and passive ion transport in alveolar epithelium. Greater than 95% of lung surface area is lined by alveolar epithelial type I (AT1) cells. Alveolar epithelial type II (AT2) cells in primary culture have been demonstrated to undergo morphologic (Cheek *et al.* 1989a) and phenotypic (Danto *et al.* 1992) transdifferentiation into AT1-like cells (Adamson and Bowden 1975; Kim *et al.* 2001a). AT1 cell-like monolayers represent a reliable model for the study of alveolar epithelial transport biology/physiology, since many of the transport processes and other characteristics demonstrated in these primary cultures appear representative of those in the respiratory epithelium lining the distal region of the intact lung (Elbert *et al.* 1999; Kim *et al.* 2001a). In this study, we utilized primary rat alveolar epithelial cell monolayers (RAECM) exhibiting AT1 cell-like phenotype (Cheek *et al.* 1989a; Danto *et al.* 1992) to investigate potential

toxicity of ultrafine ambient particle suspensions (UAPS) and several different engineered nanoparticles.

Materials and Methods

Engineered nanoparticles

Polystyrene nanoparticles (PNP) were purchased from Molecular Probes (Eugene, OR). Carboxylate-modified PNP of 20 and 100 nm diameter (-304.3 and -320 $\mu\text{Eq/g}$ surface charge, respectively) are negatively charged. Amidine-modified PNP of 20 and 120 nm diameter (80.2 and 39.7 $\mu\text{Eq/g}$ surface charge, respectively) are positively charged.

Hipco[®] single-wall carbon nanotubes (SWCNT) were purchased from Carbon Nanotechnologies (Houston, TX). SWCNT were produced by a high pressure CO conversion synthesis method (Bronikowsk et al, 2001). Individual SWCNT diameter is between 0.8 and 1.2 nm and length is between 100 and 1000 nm.

Chitosan coated (positively charged) and alginate coated (negatively charged) quantum dots (QD, 30 nm) were manufactured in our laboratories. To synthesize CdSe/ZnS QD, 25.68 mg dO (Sigma, St. Louis, MO) as precursor was used (Huang *et al.* 2004). CdO was dissolved in a coordinating solvent mixture of 3.88 mg tri-*n*-octylphosphine oxide (TOPO, Sigma) and 2.41 mg hexadecylamine (HDA, Sigma). The entire process was carried out in a dry nitrogen atmosphere. Selenium powder (31.58 mg) dissolved in 5 ml tributylphosphine (TBP, Sigma) was injected rapidly into the TOPO-CdO-HDA solution with vigorous stirring. CdSe nanocrystals were grown for 5 min at 300°C after mixing. To form a ZnS shell on the CdSe core, temperature was reduced to 160°C and a ZnS shell solution (379.4 mg zinc stearate and 12.8 mg sulfur powder dissolved in 5 mL TBP) was added into the core solution under thorough stirring over a period of 15 min. After the addition of shell solution was completed, the resulting core/shell solution was cooled to 120°C and left stirring to anneal for 2 hours. The solution was further cooled to 70°C and anhydrous methanol was added to precipitate the nanocrystals, which were collected by centrifugation and dispersed in anhydrous toluene or chloroform. To modify surface charge of QD, chitosan (Sigma) or alginate (Sigma) after grafting with hydrophobic alkyl moieties were used to encapsulate QD with average diameter of 5 nm. The size of QD coated with amphiphilic alginate or chitosan is ~30 nm by dynamic light scattering measurements (Wyatt Technology, Santa Barbara, CA).

Ultrafine ambient particulate suspensions (UAPS)

Ultrafine particle samples were collected in Los Angeles, CA in the summer. The collection site was located downwind of two major freeways (15–20 m and 150 m from the Santa Ana and Pomona Freeways, respectively). Particle samples were collected over a period of 7–10 days for 5–6 hours/day. At the end of each day's collection, samples were frozen in Teflon-lid glass jars. After one set of complete collections, multiple samples were combined and re-frozen prior to subsequent utilization in the experiments described below.

Ambient ultrafine particles were collected using the Versatile Aerosol Concentration Enrichment System (VACES) (Kim *et al.* 2001b, 2001c). Theory and operation of VACES is described in detail elsewhere (Kim *et al.* 2001b; Li *et al.* 2003). Briefly, ambient ultrafine particles were concentrated using 0.15 μm cut-point preimpaction to remove larger particles. Air samples are drawn through a saturation-condensation system that grows particles to 2–3 μm droplets, which are subsequently concentrated by virtual impaction. Highly concentrated particle suspensions were obtained by connecting the VACES output to a sterilized liquid impinger (BioSampler, SKC West, Fullerton, CA). Aerosols were collected using ultrapure

deionized water as the collection medium. Total amount of particulate loading in the collection medium was determined by multiplying the ambient concentration of each particulate population by the total air sample volume collected by each VACES line. The particle concentration in the aqueous medium was then calculated by dividing the particle loading by the total volume collected in that time period. The concentration enrichment process does not alter the physical, chemical or morphological properties of the particles (Kim *et al.* 2001b, 2001c; Li *et al.* 2003). Table 1 shows the chemical composition of UAPS utilized in this study, which contain a high percentage of organic components (mostly hydrophobic) and inorganic hydrophilic compounds such as sulfates and nitrates and a portion of trace elements and metals.

Primary culture of RAECM

The detailed procedure for routine generation of primary RAECM has appeared elsewhere (Borok *et al.* 1994; Borok *et al.* 1995). Briefly, fresh AT2 cells were isolated from adult, male, specific pathogen-free Sprague-Dawley rats (125–150 g) using elastase digestion and purification by IgG panning. Purified AT2 cells were plated onto tissue culture-treated polycarbonate filters (Transwell, 0.4 μm pore, 12 mm diameter, Corning-Costar, Cambridge, MA) at 1.2×10^6 cells/cm². Cells were maintained at 37°C in a humidified atmosphere. Culture medium (MDS) consisted of 10% newborn bovine serum in minimally of 5% CO₂/95% air. defined serum-free medium (MDSF). MDSF is a 1:1 mixture of DME/F-12 (Sigma, St. Louis, MO) supplemented with 1% nonessential amino acids (Sigma), 0.2% primocin (InvivoGen, San Diego, CA), 10 mM N-(2-hydroxyethyl)piperazine-N'-(2-ethanesulfonic acid) hemisodium salt (Sigma), 1.25 mg/mL bovine serum albumin (BD Bioscience, San Jose, CA) and 2 mM L-glutamine (Sigma). Cells were fed every other day, starting on day 3 in culture, when they form confluent monolayers.

Measurement of RAECM bioelectric properties

Transmonolayer resistance (R_t , $K\Omega\cdot\text{cm}^2$) and potential difference (PD, mV, apical side as reference) in the presence or absence of varying concentrations of apical nanoparticles were measured using a rapid screening device (Millicell-ERS, Millipore, Bedford, MA) equipped with a pair of silver/silver chloride (Ag/AgCl) electrodes (Cheek *et al.* 1989b). Short circuit current (I_{eq} , $\mu\text{A}/\text{cm}^2$) was calculated according to Ohm's law as described previously. Immediately before and at different time points after apical exposure to nanoparticles, R_t and PD were measured and I_{eq} calculated.

Apical exposure of RAECM to nanoparticles

We studied the effects of apical exposure to nanoparticles by replacing monolayer apical fluid on days 4, 5 or 6 in culture with isotonic solutions of UAPS, PNP, QD or SWCNT. UAPS in water were adjusted to isosmolarity using NaCl. PNP, QD and SWCNT were suspended in MDS. These working stocks were sonicated briefly and appropriate volume was used to replace apical fluid. Apical fluid of control RAECM was replaced at the same time as experimental RAECM using MDS or isosmolar NaCl solution without nanoparticles. Effects of UAPS, PNP, QD and SWCNT concentrations of up to 36, 706, 176 and 88 $\mu\text{g}/\text{mL}$, respectively, were studied. In some experiments, monolayers were apically exposed for 120 min to UAPS (9 $\mu\text{g}/\text{mL}$), followed by replacement of apical fluid with fresh culture medium. R_t and I_{eq} were usually assessed at 15, 30, 60, 120, 240 and 1440 min. Furthermore, permeabilities of ¹⁴C-mannitol (180 Da) and ¹⁴C-inulin (~5000 Da) were estimated from their steady state fluxes across RAECM in the apical-to-basolateral direction in the presence or absence of UAPS (36 $\mu\text{g}/\text{mL}$). Five μL of radiotracer amounts of either mannitol or inulin were added immediately after monolayer apical UAPS exposure. Fifty μL samples of basolateral fluid were taken at 30, 60, 120, 240 and 1440 min after radiotracer

instillation into apical fluid. Ten μL samples were taken from apical fluid at 60 and 1440 min for determination of upstream radioactivity. Radioactive samples were mixed with 15 mL Ecoscint (National Diagnostics, Atlanta, GA) and assayed using a beta counter (Beckman Instruments, Fullerton, CA).

Measurement of lactate dehydrogenase (LDH) release

Extracellular LDH (in apical and basolateral fluid) at 1 and 2 hours after exposure to UAPS (18 $\mu\text{g}/\text{mL}$) or SWCNT (88 $\mu\text{g}/\text{mL}$) was measured using a colorimetric cytotoxicity detection kit (Roche, Indianapolis, IN) following the manufacturer's instructions. As control, release of LDH was obtained for unexposed cells (low control) and maximum release of LDH was obtained by lysis of cells with 0.2% TX-100 (high control). Cytotoxicity is defined by:

$$\frac{(\text{release of LDH of exposed cells} - \text{release of LDH (low control)})}{(\text{release of LDH (high control)} - \text{release of LDH (low control)})}$$

Statistical Analyses

Data are presented as mean \pm standard error. For comparisons of multiple group means, one-way or two-way analyses of variance (ANOVA) followed by post-hoc procedures based on modified Newman-Keuls-Student tests were performed using GB-stat v9.0 software (Dynamic Microsystems, Silver Spring, MD). $P < 0.05$ was considered to be statistically significant.

Results

Time courses of changes in R_t following apical exposure of RAECM to UAPS are shown in Figure 1. Average R_t of RAECM before UAPS exposure was $1.41 \pm 0.05 \text{ K}\Omega\cdot\text{cm}^2$ ($n = 45$). At the highest UAPS concentration (36 $\mu\text{g}/\text{mL}$) studied, R_t declined $\sim 60\%$ with half time of ~ 30 min. From 2 to 24 hours, no further significant changes in R_t were observed, despite continued presence of UAPS in apical fluid. No significant changes in cytotoxicity compared to controls were observed after 1 and 2 hours of monolayer exposure to 18 $\mu\text{g}/\text{mL}$ UAPS ($n = 5$, data not shown).

Figure 2 shows the effects of apical UAPS on I_{eq} . I_{eq} prior to UAPS exposure was $4.72 \pm 0.10 \mu\text{A}/\text{cm}^2$ ($n = 45$). At the highest apical UAPS concentration (36 $\mu\text{g}/\text{mL}$) studied, I_{eq} decreased by $\sim 25\%$ at 2 hours. From 2 to 24 hours, no further significant changes in I_{eq} were observed, despite the continued presence of UAPS in apical fluid.

Figure 3 shows time courses of changes in R_t of RAECM exposed apically to 9 $\mu\text{g}/\text{mL}$ UAPS for 2 hours, followed by replacement of apical fluid with fresh culture medium. R_t prior to UAPS exposure was $2.33 \pm 0.68 \text{ K}\Omega\cdot\text{cm}^2$ ($n = 3$). R_t recovered toward control after replacing apical fluid with fresh culture medium. Washout caused an increase in I_{eq} , followed by a gradual return toward its initial value (data not shown). I_{eq} prior to UAPS exposure was $5.29 \pm 1.55 \mu\text{A}/\text{cm}^2$ ($n = 3$).

Apparent permeabilities (P_{app}) of ^{14}C -mannitol and ^{14}C -inulin measured in the presence and absence of apical exposure to UAPS (36 $\mu\text{g}/\text{mL}$) are summarized in Table 2. P_{app} of neither ^{14}C -mannitol nor ^{14}C -inulin measured in the apical-to-basolateral direction was significantly altered by UAPS exposure.

Time courses of changes in R_t following apical exposure of RAECM to positively or negatively charged QD (176 $\mu\text{g}/\text{mL}$) are shown in Figure 4. Average R_t before QD exposure was $2.68 \pm 0.14 \text{ K}\Omega\cdot\text{cm}^2$ ($n = 10$). Positively charged QD decreased R_t by ~60% after 2 hours of exposure, while negatively charged QD did not decrease R_t significantly. Effects of these two types of QD on I_{eq} were not significantly different from control over 24 hours (data not shown). Lower concentrations (44–88 $\mu\text{g}/\text{mL}$) of QD (positively or negatively charged) did not decrease R_t significantly over 24 hours of exposure (data not shown).

Time courses of changes in R_t following apical exposure of RAECM to SWCNT (up to 88 $\mu\text{g}/\text{mL}$) are shown in Figure 5. Average R_t before SWCNT exposure was $3.24 \pm 0.07 \text{ K}\Omega\cdot\text{cm}^2$ ($n = 33$). R_t decreased significantly compared to control monolayers by ~40% after 1 hour of exposure, with recovery to initial value by 4 to 24 hours. The decrease in R_t after exposure to SWCNT was not dose dependent. Effects of SWCNT (up to 88 $\mu\text{g}/\text{mL}$) on I_{eq} were not significantly different from control for up to 24 hours of exposure (data not shown). No significant changes in cytotoxicity were observed after 1 and 2 hours of monolayer exposure to 88 $\mu\text{g}/\text{mL}$ SWCNT ($n=5$, data not shown).

Figure 6 shows the time courses of R_t observed for PNP (176 $\mu\text{g}/\text{mL}$) exposure. RAECM prior to PNP exposure show average $R_t = 3.58 \pm 0.11 \text{ K}\Omega\cdot\text{cm}^2$ and average $I_{\text{eq}} = 4.48 \pm 0.16 \mu\text{A}/\text{cm}^2$ ($n = 47$). No significant changes were observed for 20 nm positively and negatively charged PNP or for 100 nm negatively and 120 nm positively (data not shown) charged PNP. Up to 706 $\mu\text{g}/\text{mL}$ of PNP in apical fluid led to no significant changes in R_t or I_{eq} for up to 24 hours (data not shown), and 176 $\mu\text{g}/\text{mL}$ PNP in apical fluid led to no significant changes in R_t or I_{eq} for up to 6 days (data not shown).

Figure 7 summarizes changes in R_t after 2, 4 and 24 hours of exposure to 36 $\mu\text{g}/\text{mL}$ of UAPS, 176 $\mu\text{g}/\text{mL}$ QD (positively and negatively charged), 88 $\mu\text{g}/\text{mL}$ SWCNT and PNP (20 and 100 nm negatively charged and 20 nm positively charged). Average R_t of RAECM before nanoparticle exposure was $2.13 \pm 0.27 \text{ K}\Omega\cdot\text{cm}^2$ ($n = 66$). Exposure of RAECM to different nanoparticles affects R_t differently due to different nanoparticle composition, charge and/or concentration used.

Discussion

In this study, we demonstrate that effects of ambient ultrafine particles and engineered nanoparticles on barrier properties of RAECM are strongly dependent on nanoparticle composition, charge and/or concentration. Exposure to UAPS (up to 36 $\mu\text{g}/\text{mL}$) decreased R_t and I_{eq} over time significantly, while PNP (negatively and positively charged, up to 706 $\mu\text{g}/\text{mL}$) did not affect R_t or I_{eq} . After 1 hour of RAECM exposure to SWCNT (up to 88 $\mu\text{g}/\text{mL}$), R_t decreased significantly but transiently, recovering to initial values after 4–24 hours. Exposure to positively charged QD (176 $\mu\text{g}/\text{mL}$) decreased R_t significantly, but negatively charged QD (up to 176 $\mu\text{g}/\text{mL}$) and lower concentrations of positively charged QD (44 and 88 $\mu\text{g}/\text{mL}$) had no effect on R_t and I_{eq} .

Analysis of UAPS composition (Table 1) revealed a high percentage of organic components (mostly hydrophobic) and inorganic hydrophilic compounds (sulfates, nitrates and trace elements and metals). Despite these data on composition, properties of UAPS remain complex and ill-defined. Due to this complexity, the mechanisms of UAPS toxicity remain obscure. Disruption of lung alveolar epithelial barrier properties may be caused by multiple factors associated with UAPS, including trace elements and metals, elemental and/or organic carbon content and large overall particle surface area (Oberdorster *et al.* 2005b). Ultrafine particles may also act as a catalyst for endogenous effects on lung epithelium, leading to increased toxicity and inflammation (Oberdorster 2001). The larger surface afforded by

ultrafine particles compared to larger particles may increase particle surface-dependent reactions (e.g., generation of reactive oxidant species) (Ibald-Mulli *et al.* 2002; Wichmann *et al.* 2000). Lack of effects of UAPS on paracellular movement of hydrophilic solutes suggests that the observed decreases in R_t and I_{eq} in response to apical UAPS exposure of monolayers reflect primarily changes in transcellular transport properties (e.g., ion channel and pump activities), consistent with the absence of cytotoxicity (no increase in LDH release) after UAPS exposure.

In related studies, ultrafine carbon black particles were reported to cause detectable proinflammatory effects in rat lung, including modest neutrophil influx, protein leak, and modulation of glutathione levels (Donaldson *et al.* 2001). Ultrafine particles made of low-solubility and low-toxicity materials were found to be inflammatory in rat lung (Donaldson *et al.* 2002). Aerosolized ultrafine TiO_2 particles were shown to cause severe bronchoalveolar inflammation (Ferin *et al.* 1992). Instillation of ultrafine carbon black particles (~14 nm) intratracheally into rat lungs led to a marked increase in lactate dehydrogenase (LDH) levels in bronchoalveolar lavage (BAL) fluid (Li *et al.* 1999). Intratracheal instillation of diesel exhaust particles (~30 nm) and an amorphous silicon dioxide (commercially available as Carbosil, ~7 nm) into lungs of male Sprague-Dawley rats increased air-blood barrier permeability, inflammation and edema formation, leading to a strong correlation of plasma viscosity with an index of type I cell injury (reflected as rat type I cell marker found in lung lavage fluid) (Evans *et al.* 2006). By contrast, healthy mice did not appear to respond to ultrafine carbon and platinum particles (15 and 25 nm, respectively) when inhaled for up to 6 hours at 110 $\mu\text{g}/\text{mL}$ (Oberdorster 2001). These effects may be dependent on many factors, including physicochemical characteristics of particles. Health effects manifested by ambient particulates are currently thought to be especially important in specific risk groups of persons who are predisposed to injury by genetic susceptibility, age and/or disease (Kreyling *et al.* 2006).

QD toxicity appears to be dependent on particle size, charge, concentration and surface coating bioactivity (Derfus *et al.* 2003; Hardman 2006; Hoshino *et al.* 2004; Zhang *et al.* 2006). Our results show that positively charged QD are more toxic to RAECM compared to negatively charged QD. Cationic amino acids and peptides are known to increase leakage of solutes into alveolar fluid by disruption of tight junctional pathways (Kim and Malik 2003), suggesting that positively charged nanoparticles may cause injury to air-blood barriers of the lung by related mechanisms. Uncoated QD made of core/shell CdSe/ZnS have been reported to be toxic to cells due to surface oxidation which, through a variety of pathways, leads to release Cd^{2+} ions into the cellular environment (Derfus *et al.* 2003; Zhang *et al.* 2006). Studies of toxicity of QD with different coatings (neutral, negatively or positively charged) in primary human epidermal keratinocytes showed that negatively and positively charged QD were both toxic up to 20 nM, while neutral QD were not, after 48 hours of exposure (Ryman-Rasmussen *et al.* 2007). These varying results suggest that QD cytotoxicity depends at least in part on specific cellular interactions and particle physicochemical properties.

Our results suggest that SWCNT acutely and transiently affect passive barrier properties, without appreciably affecting active ion transport properties of the alveolar epithelial barrier. Manufactured SWCNT may contain significant amounts of metallic impurities that can serve as catalysts for oxidative stress. The specific physicochemical properties and metallic content (especially iron) of SWCNT may have contributed to the observed effects. After intratracheal instillation in mice (Lam *et al.* 2004) and rats (Warheit *et al.* 2004), unpurified and/or purified SWCNT caused epithelial granulomatous reactions. In another study, it was shown that purified SWCNT induce acute inflammatory reactions and decreased bacterial clearance in rats (Shvedova *et al.* 2005). Unpurified SWCNT exposure led to generation of reactive oxygen species and increased oxidant stress and cytotoxicity in human bronchial

epithelial cells (Shvedova *et al.* 2003). Other studies showed purified and/or unpurified SWCNT causes very low toxicity to the rat alveolar cell line NR8383 (Pulskamp *et al.* 2007) and human alveolar epithelial cell line A549 (Davoren *et al.* 2006; Pulskamp *et al.* 2007). It has been reported that iron content of enriched SWCNT has a significantly more pronounced toxic effect on cultured cell lines (human keratinocytes) than SWCNT treated with iron chelators (Shvedova *et al.* 2003), consistent with the possibility that metal impurities in SWCNT preparations may be more damaging to cells than SWCNT themselves (Shvedova *et al.* 2003).

Our studies demonstrate that apical exposure of RAECM to concentrations up to 706 µg/mL of positively and negatively charged PNP (20, 100 and 120 nm) cause no significant changes in active and passive transport properties over 24 hours. These findings are in agreement with a recent preliminary report using 46 nm PNP (positive or negative surface charge) in isolated primary rat AT2 cells (Geys *et al.* 2006). On the other hand, studies with a phagocytic cell line (RAW 264.7) showed that positively charged PNP (60 nm) produces reactive oxygen species, mitochondrial damage and cellular toxicity (although negatively charged PNP have little effect (Xia *et al.* 2006)), while studies in rat lungs *in vivo* showed that instillation of 64 nm PNP (1 mg) caused significant cell death as measured by BAL LDH levels (Brown *et al.* 2001). These data suggest that cellular toxicity of PNP may be related at least in part to the specific cell types and experimental milieu in which exposure occurs.

In summary, we have shown that UAPS, QD and SWCNT (but not PNP) can alter the active and/or passive ion transport properties of primary RAECM. We conclude that physicochemical properties of nanoparticles, a result of their varying sources, formation mechanisms, composition or surface charge, are important factors in determining their effects on lung alveolar epithelial barrier properties. Further mechanistic studies with defined nanoparticles may provide additional insights into how nanoparticles interact with alveolar epithelial cells and lead to modulation of barrier properties.

Acknowledgments

The authors appreciate the technical assistance of Juan Raymond Alvarez. E. D. Crandall is Hastings Professor and Kenneth T. Norris Jr. Chair of Medicine. This work was supported in part by the Hastings Foundation, research grants HL 38578, HL 38621, HL 38658, HL 62569 and HL 64365 from the National Institutes of Health, and the Southern California Particle Center and Supersite (SCPCS) funded by the Environmental Protection Agency (EPA) under the STAR Program. Research described herein has not been subjected to the EPA required peer and policy review and therefore does not necessarily reflect the views of EPA, and no official endorsement should be inferred. Mention of trade names or commercial products does not constitute an endorsement or recommendation for use.

References

- Adamson IY, Bowden DH. Derivation of type 1 epithelium from type 2 cells in the developing rat lung. *Laboratory Investigation*. 1975; 32:736–45. [PubMed: 1171339]
- Alfaro-Moreno E, Martinez L, Garcia-Cuellar C, Bonner JC, Murray JC, Rosas I, Rosales SP, Osornio-Vargas AR. Biologic effects induced *in vitro* by PM10 from three different zones of Mexico City. *Environmental Health Perspectives*. 2002; 110:715–20. [PubMed: 12117649]
- Borok Z, Danto SI, Zabski SM, Crandall ED. Defined medium for primary culture *de novo* of adult rat alveolar epithelial cells. *In Vitro Cellular & Developmental Biology. Animal*. 1994; 30A:99–104.
- Borok Z, Hami A, Danto SI, Zabski SM, Crandall ED. Rat serum inhibits progression of alveolar epithelial cells toward the type I cell phenotype *in vitro*. *American Journal of Respiratory Cell and Molecular Biology*. 1995; 12:50–5. [PubMed: 7811470]
- Brown DM, Wilson MR, MacNee W, Stone V, Donaldson K. Size-dependent proinflammatory effects of ultrafine polystyrene particles: a role for surface area and oxidative stress in the enhanced activity of ultrafines. *Toxicology and Applied Pharmacology*. 2001; 175:191–9. [PubMed: 11559017]

- Calcabrini A, Meschini S, Marra M, Falzano L, Colone M, De Berardis B, Paoletti L, Arancia G, Fiorentini C. Fine environmental particulate engenders alterations in human lung epithelial A549 cells. *Environmental Research*. 2004; 95:82–91. [PubMed: 15068934]
- Cassee FR, Muijser H, Duistermaat E, Freijer JJ, Geerse KB, Marijnissen JC, Arts JH. Particle size-dependent total mass deposition in lungs determines inhalation toxicity of cadmium chloride aerosols in rats. Application of a multiple path dosimetry model. *Archives of Toxicology*. 2002; 76:277–86. [PubMed: 12107645]
- Cheek JM, Evans MJ, Crandall ED. Type I cell-like morphology in tight alveolar epithelial monolayers. *Experimental Cell Research*. 1989a; 184:375–87. [PubMed: 2806398]
- Cheek JM, Kim KJ, Crandall ED. Tight monolayers of rat alveolar epithelial cells: bioelectric properties and active sodium transport. *American Journal of Physiology*. 1989b; 256:C688–93. [PubMed: 2923201]
- Danto SI, Zabski SM, Crandall ED. Reactivity of alveolar epithelial cells in primary culture with type I cell monoclonal antibodies. *American Journal of Respiratory Cell and Molecular Biology*. 1992; 6:296–306. [PubMed: 1540393]
- Davoren M, Herzog E, Casey A, Cottineau B, Chambers G, Byrne HJ, Lyng FM. In vitro toxicity evaluation of single walled carbon nanotubes on human A549 lung cells. *Toxicology In Vitro*. 2006 Article in Press.
- Derfus AM, Chan WCW, Bhatia SN. Probing the Cytotoxicity of Semiconductor Quantum Dots. *Nano Letters*. 2003; 4:11–8.
- Donaldson K, Brown D, Clouter A, Duffin R, MacNee W, Renwick L, Tran L, Stone V. The pulmonary toxicology of ultrafine particles. *Journal of Aerosol Medicine*. 2002; 15:213–20. [PubMed: 12184871]
- Donaldson K, Stone V, Clouter A, Renwick L, MacNee W. Ultrafine particles. *Occupational and Environmental Medicine*. 2001; 58(211–6):199.
- Elbert KJ, Schafer UF, Schafers HJ, Kim KJ, Lee VH, Lehr CM. Monolayers of human alveolar epithelial cells in primary culture for pulmonary absorption and transport studies. *Pharmaceutical Research*. 1999; 16:601–8. [PubMed: 10349999]
- Evans SA, Al-Mosawi A, Adams RA, Berube KA. Inflammation, edema, and peripheral blood changes in lung-compromised rats after instillation with combustion-derived and manufactured nanoparticles. *Experimental Lung Research*. 2006; 32:363–78. [PubMed: 17090477]
- Ferin J, Oberdorster G, Penney DP. Pulmonary retention of ultrafine and fine particles in rats. *American Journal of Respiratory Cell and Molecular Biology*. 1992; 6:535–42. [PubMed: 1581076]
- Geys J, Coenegrachts L, Vercammen J, Engelborghs Y, Nemmar A, Nemery B, Hoet PH. In vitro study of the pulmonary translocation of nanoparticles: a preliminary study. *Toxicology Letters*. 2006; 160:218–26. [PubMed: 16137845]
- Ghio AJ, Devlin RB. Inflammatory lung injury after bronchial instillation of air pollution particles. *American Journal of Respiratory and Critical Care Medicine*. 2001; 164:704–8. [PubMed: 11520740]
- Gurr JR, Wang AS, Chen CH, Jan KY. Ultrafine titanium dioxide particles in the absence of photoactivation can induce oxidative damage to human bronchial epithelial cells. *Toxicology*. 2005; 213:66–73. [PubMed: 15970370]
- Gutierrez-Castillo ME, Roubicek DA, Cebrian-Garcia ME, De Vizcaya-Ruiz A, Sordo-Cedeno M, Ostrosky-Wegman P. Effect of chemical composition on the induction of DNA damage by urban airborne particulate matter. *Environmental and Molecular Mutagenesis*. 2006; 47:199–211. [PubMed: 16355389]
- Hardman R. A toxicologic review of quantum dots: toxicity depends on physicochemical and environmental factors. *Environmental Health Perspectives*. 2006; 114:165–72. [PubMed: 16451849]
- Hoshino A, Fujioka K, Oku T, Nakamura S, Suga M, Yamaguchi Y, Suzuki K, Yasuhara M, Yamamoto K. Quantum dots targeted to the assigned organelle in living cells. *Microbiology and Immunology*. 2004; 48:985–94. [PubMed: 15611617]

- Huang GW, Chen CY, Wu KC, Ahmed MO, Chou PT. One-pot synthesis and characterization of high-quality CdSe/ZnX (X=S, Se) nanocrystals via the CdO precursor. *Journal of Crystal Growth*. 2004; 265:250–9.
- Ibald-Mulli A, Wichmann HE, Kreyling W, Peters A. Epidemiological evidence on health effects of ultrafine particles. *Journal of Aerosol Medicine*. 2002; 15:189–201. [PubMed: 12184869]
- Kim KJ, Borok Z, Crandall ED. A useful in vitro model for transport studies of alveolar epithelial barrier. *Pharmaceutical Research*. 2001a; 18:253–5. [PubMed: 11442260]
- Kim KJ, Malik AB. Protein transport across the lung epithelial barrier. *American Journal of Physiology*. 2003; 284:L247–59. [PubMed: 12533309]
- Kim S, Jaques PA, Chang M, Froines JR, Sioutas C. Versatile aerosol concentration enrichment system (VACES) for simultaneous in vivo and in vitro evaluation of toxic effects of ultrafine, fine and coarse ambient particles. Part I: Development and laboratory characterization. *Journal of Aerosol Science*. 2001b; 32:1281–97.
- Kim S, Jaques PA, Chang M, Froines JR, Sioutas C. Versatile aerosol concentration enrichment system (VACES) for simultaneous in vivo and in vitro evaluation of toxic effects of ultrafine, fine and coarse ambient particles. Part II: Field evaluation. *Journal of Aerosol Science*. 2001c; 32:1299–1314.
- Kreyling WG, Semmler-Behnke M, Moller W. Ultrafine particle-lung interactions: does size matter? *Journal of Aerosol Medicine*. 2006; 19:74–83. [PubMed: 16551218]
- Lam C, James JT, McCluskey R, Hunter RL. Pulmonary Toxicity of Single-Wall Carbon Nanotubes in Mice 7 and 90 Days After Intratracheal Instillation. *Respiratory toxicology*. 2004; 77:126–34.
- Li N, Sioutas C, Cho A, Schmitz D, Misra C, Sempf J, Wang M, Oberley T, Froines J, Nel A. Ultrafine particulate pollutants induce oxidative stress and mitochondrial damage. *Environmental Health Perspectives*. 2003; 111:455–60. [PubMed: 12676598]
- Li XY, Brown D, Smith S, MacNee W, Donaldson K. Short-term inflammatory responses following intratracheal instillation of fine and ultrafine carbon black in rats. *Inhalation Toxicology*. 1999; 11:709–31. [PubMed: 10477444]
- Magrez A, Kasas S, Salicio V, Pasquier N, Seo JW, Celio M, Catsicas S, Schwaller B, Forro L. Cellular toxicity of carbon-based nanomaterials. *Nano Letters*. 2006; 6:1121–5. [PubMed: 16771565]
- Monn C, Becker S. Cytotoxicity and induction of proinflammatory cytokines from human monocytes exposed to fine (PM_{2.5}) and coarse particles (PM_{10-2.5}) in outdoor and indoor air. *Toxicology and Applied Pharmacology*. 1999; 155:245–52. [PubMed: 10079210]
- Muldoon LL, Sandor M, Pinkston KE, Neuwelt EA. Imaging, distribution, and toxicity of superparamagnetic iron oxide magnetic resonance nanoparticles in the rat brain and intracerebral tumor. *Neurosurgery*. 2005; 57:785–96. [PubMed: 16239893]
- Nemmar A, Hoet PH, Vanquickenborne B, Dinsdale D, Thomeer M, Hoylaerts MF, Vanbilloen H, Mortelmans L, Nemery B. Passage of inhaled particles into the blood circulation in humans. *Circulation*. 2002; 105:411–4. [PubMed: 11815420]
- Nemmar A, Vanbilloen H, Hoylaerts MF, Hoet PH, Verbruggen A, Nemery B. Passage of intratracheally instilled ultrafine particles from the lung into the systemic circulation in hamster. *American Journal of Respiratory and Critical Care Medicine*. 2001; 164:1665–8. [PubMed: 11719307]
- Oberdorster G. Pulmonary effects of inhaled ultrafine particles. *International Archives of Occupational and Environmental Health*. 2001; 74:1–8. [PubMed: 11196075]
- Oberdorster G, Gelein RM, Ferin J, Weiss B. Association of particulate air pollution and acute mortality: involvement of ultrafine particles? *Inhalation Toxicology*. 1995; 7:111–24. [PubMed: 11541043]
- Oberdorster G, Maynard A, Donaldson K, Castranova V, Fitzpatrick J, Ausman K, Carter J, Karn B, Kreyling W, Lai D, Olin S, Monteiro-Riviere N, Warheit D, Yang H. Principles for characterizing the potential human health effects from exposure to nanomaterials: elements of a screening strategy. *Particle and Fibre Toxicology*. 2005a; 2:8. [PubMed: 16209704]

- Oberdorster G, Oberdorster E, Oberdorster J. Nanotoxicology: an emerging discipline evolving from studies of ultrafine particles. *Environmental Health Perspectives*. 2005b; 113:823–39. [PubMed: 16002369]
- Osornio-Vargas AR, Bonner JC, Alfaro-Moreno E, Martinez L, Garcia-Cuellar C, Ponce-de-Leon Rosales S, Miranda J, Rosas I. Proinflammatory and cytotoxic effects of Mexico City air pollution particulate matter in vitro are dependent on particle size and composition. *Environmental Health Perspectives*. 2003; 111:1289–93. [PubMed: 12896848]
- Peters A, Dockery DW, Muller JE, Mittleman MA. Increased particulate air pollution and the triggering of myocardial infarction. *Circulation*. 2001; 103:2810–5. [PubMed: 11401937]
- Pulskamp K, Diabate S, Krug HF. Carbon nanotubes show no sign of acute toxicity but induce intracellular reactive oxygen species in dependence on contaminants. *Toxicology Letters*. 2007; 168:58–74. [PubMed: 17141434]
- Ryman-Rasmussen JP, Riviere JE, Monteiro-Riviere NA. Surface coatings determine cytotoxicity and irritation potential of quantum dot nanoparticles in epidermal keratinocytes. *Journal of Investigative Dermatology*. 2007; 127:143–53. [PubMed: 16902417]
- Sayes CM, Liang F, Hudson JL, Mendez J, Guo W, Beach JM, Moore VC, Doyle CD, West JL, Billups WE, Ausman KD, Colvin VL. Functionalization density dependence of single-walled carbon nanotubes cytotoxicity in vitro. *Toxicology Letters*. 2006; 161:135–42. [PubMed: 16229976]
- Shvedova AA, Castranova V, Kisin ER, Schwegler-Berry D, Murray AR, Gandelsman VZ, Maynard A, Baron P. Exposure to carbon nanotube material: assessment of nanotube cytotoxicity using human keratinocyte cells. *Journal of Toxicology and Environmental Health. Part A*. 2003; 66:1909–26. [PubMed: 14514433]
- Shvedova AA, Kisin ER, Mercer R, Murray AR, Johnson VJ, Potapovich AI, Tyurina YY, Gorelik O, Arepalli S, Schwegler-Berry D, Hubbs AF, Antonini J, Evans DE, Ku BK, Ramsey D, Maynard A, Kagan VE, Castranova V, Baron P. Unusual inflammatory and fibrogenic pulmonary responses to single-walled carbon nanotubes in mice. *American Journal of Physiology*. 2005; 289:L698–708. [PubMed: 15951334]
- Sun Q, Wang A, Jin X, Natanzon A, Duquaine D, Brook RD, Aguinaldo JG, Fayad ZA, Fuster V, Lippmann M, Chen LC, Rajagopalan S. Long-term air pollution exposure and acceleration of atherosclerosis and vascular inflammation in an animal model. *JAMA : Journal of the American Medical Association*. 2005; 294:3003–10.
- Topinka J, Schwarz LR, Wiebel FJ, Cerna M, Wolff T. Genotoxicity of urban air pollutants in the Czech Republic. Part II. DNA adduct formation in mammalian cells by extractable organic matter. *Mutation Research*. 2000; 469:83–93. [PubMed: 10946245]
- Vedal S. Ambient particles and health: lines that divide. *Journal of the Air & Waste Management Association*. 1997; 47:551–81. [PubMed: 9155246]
- Warheit DB, Laurence BR, Reed KL, Roach DH, Reynolds GA, Webb TR. Comparative pulmonary toxicity assessment of single-wall carbon nanotubes in rats. *Toxicological Sciences*. 2004; 77:117–25. [PubMed: 14514968]
- Wichmann, HE.; Spix, C.; Tuch, T.; Wolke, G.; Peters, A.; Heinrich, J.; Kreyling, WG.; Heyder, J. Research Report (Health Effects Institute). 2000. Daily mortality and fine and ultrafine particles in erfurt, germany part I: role of particle number and particle mass; p. 5-86.discussion 87–94
- Xia T, Kovochich M, Brant J, Hotze M, Sempf J, Oberley T, Sioutas C, Yeh JI, Wiesner MR, Nel AE. Comparison of the abilities of ambient and manufactured nanoparticles to induce cellular toxicity according to an oxidative stress paradigm. *Nano Letters*. 2006; 6:1794–807. [PubMed: 16895376]
- Zhang T, Stilwell JL, Gerion D, Ding L, Elboudwarej O, Cooke PA, Gray JW, Alivisatos AP, Chen FF. Cellular effect of high doses of silica-coated quantum dot profiled with high throughput gene expression analysis and high content cellomics measurements. *Nano Letters*. 2006; 6:800–8. [PubMed: 16608287]

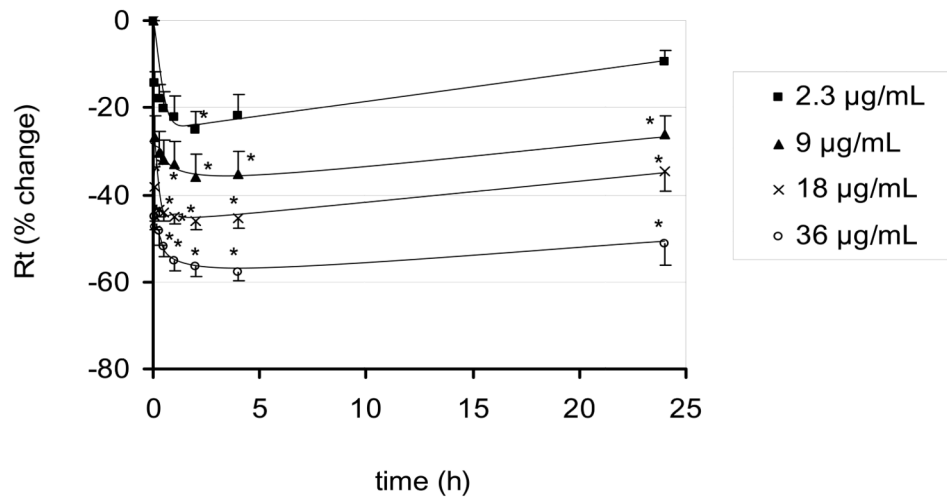


Figure 1. Effects of apical exposure to UAPS on Rt of RAECM (n = 4–9 for each concentration). Rt of all monolayers prior to apical UAPS exposure (at t = 0) was $1.41 \pm 0.05 \text{ K}\Omega\cdot\text{cm}^2$ (n = 45). At the maximum concentration of UAPS (36 $\mu\text{g}/\text{mL}$) studied, Rt declined significantly by 60% after 2 hours of exposure and did not change further over 24 hours. * = significantly different ($p < 0.05$) from control (monolayers not exposed to UAPS).

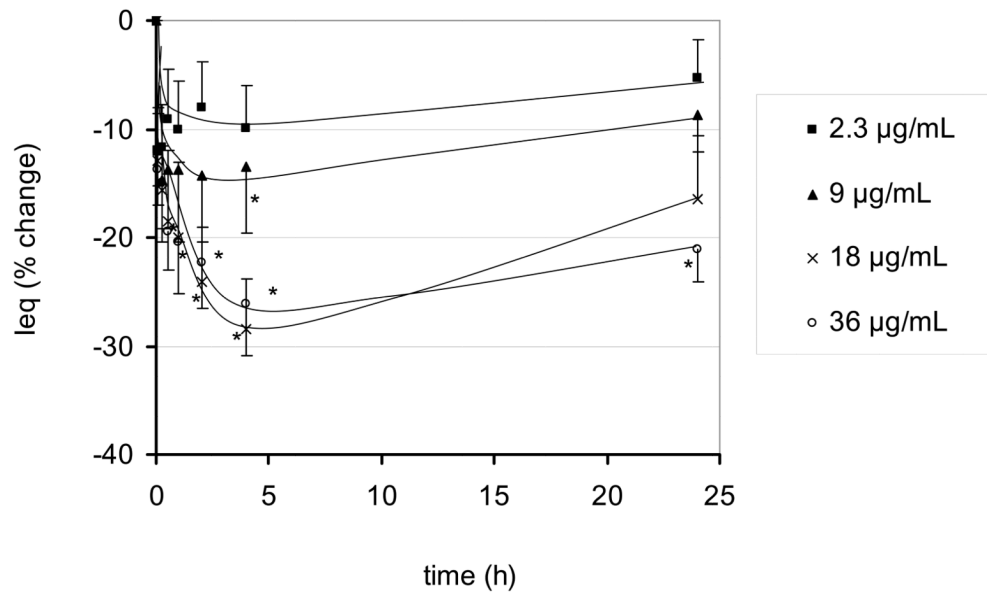


Figure 2. Effects of apical exposure to UAPS on Ieq of RAECM (n = 4–9 for each concentration). Ieq of all monolayers prior to apical UAPS exposure of (at t = 0) was $4.72 \pm 0.10 \mu\text{A}/\text{cm}^2$ (n = 45). At the maximum concentration of UAPS (36 $\mu\text{g}/\text{mL}$) studied, Ieq declined significantly by ~25% after 30 min of exposure and did not change further for up to 24 hours. * = significantly different ($p < 0.05$) from control (monolayers not exposed to UAPS).

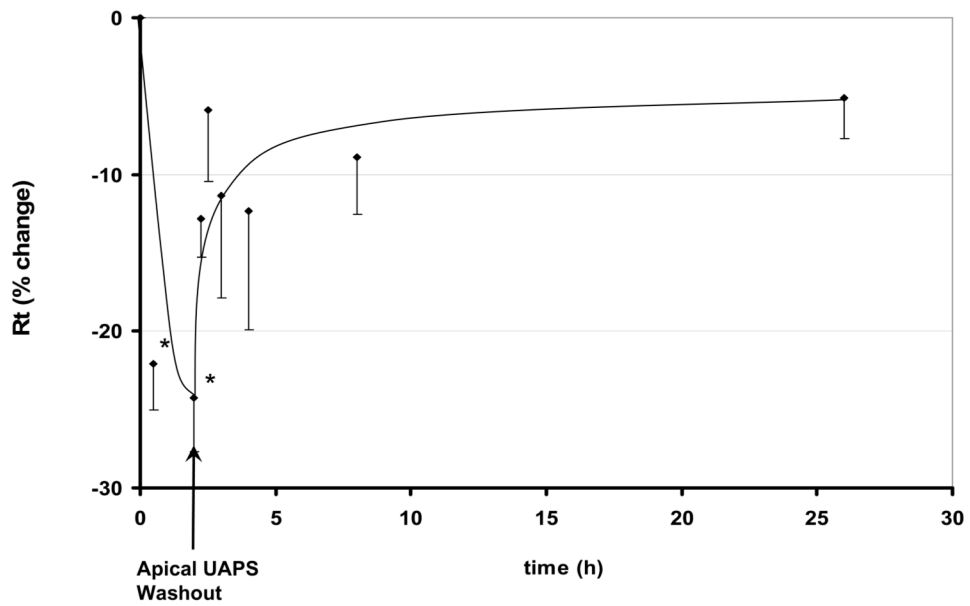


Figure 3. Effects of removal of apical UAPS (9 $\mu\text{g/mL}$) on Rt of RAECM after 2 hours of exposure. Rt prior to apical exposure to UAPS ($t = 0$) was $2.33 \pm 0.68 \text{ K}\Omega\cdot\text{cm}^2$ ($n = 3$). After 1 and 2 hours of UAPS exposure, Rt decreased significantly. Rt after replacement of UAPS with fresh culture medium recovered toward control values. * = significantly different ($p < 0.05$) from control (monolayers not exposed to UAPS).

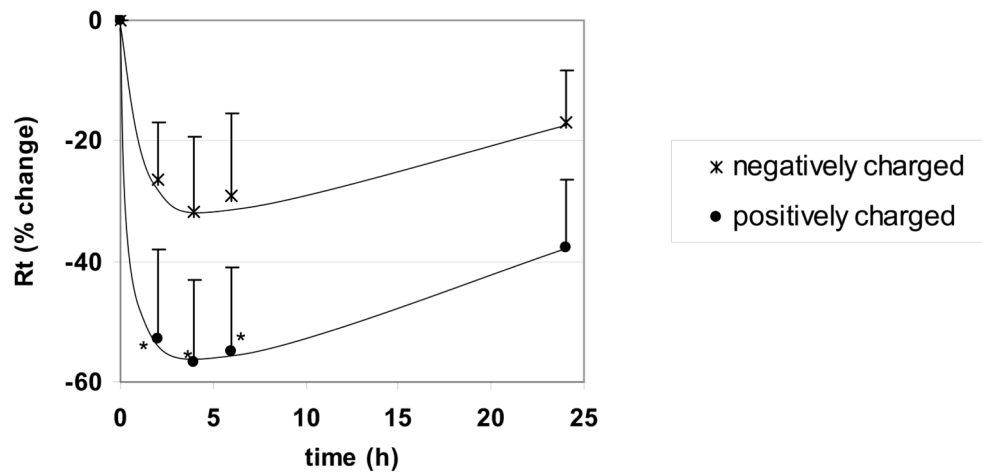


Figure 4. Effects of apical exposure to QD (176 $\mu\text{g}/\text{mL}$) on Rt of RAECM ($n = 6$ for each concentration). Rt of all monolayers prior to apical exposure to QD (at $t = 0$) was $2.68 \pm 0.14 \text{ K}\Omega.\text{cm}^2$ ($n = 19$). Exposure to positively charged QD decreased Rt significantly after 1 hour, with recovery to control level by 24 hours. * = significantly different ($p < 0.05$) from control (monolayers not exposed to QD).

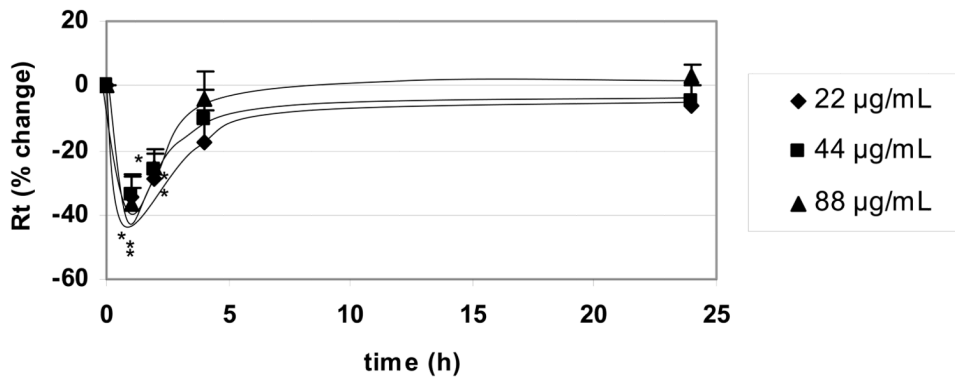


Figure 5.

Effects of apical exposure to SWCNT on Rt of RAECM (n = 9 for each concentration). Rt of all monolayers used prior to apical exposure to SWCNT (at t = 0) was 3.24 ± 0.07 $\text{K}\Omega\cdot\text{cm}^2$ (n = 33). Exposure to SWCNT up to 88 $\mu\text{g}/\text{mL}$ decreased Rt significantly after 1 hour. Rt recovered to control level by 4–24 hours. * = significantly different ($p < 0.05$) from control (monolayers not exposed to SWCNT).

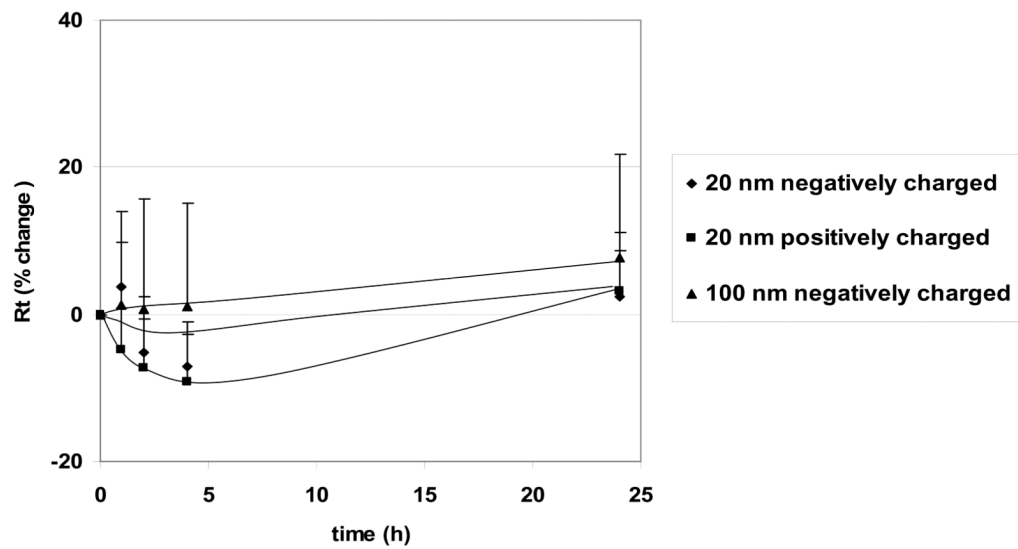


Figure 6. Effects of apical exposure to PNP (176 $\mu\text{g/mL}$, 20 nm positively and negatively charged and 100 nm negatively charged) on R_t of RAECM ($n = 10\text{--}13$ for each concentration). R_t of all monolayers prior to apical exposure to PNP (at $t = 0$) was $3.58 \pm 0.11 \text{ K}\Omega\text{cm}^2$ ($n = 47$). These three types of PNP, as well as positively charged 120 nm PNP (data not shown), did not cause significant changes in R_t or I_{eq} (data not shown).

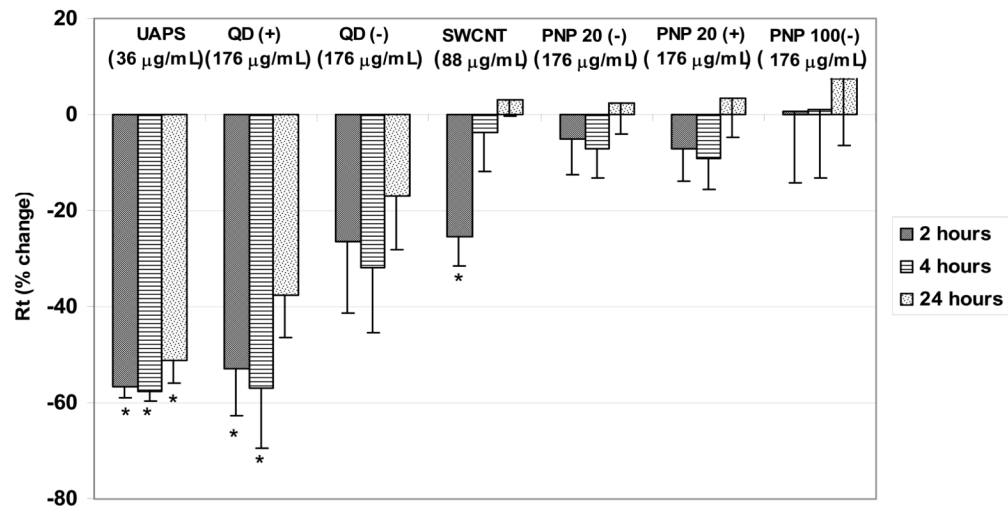


Figure 7.

Effects of apical exposure to UAPS (36 µg/mL), SWCNT (88 µg/mL), QD (positively and negatively charged, 176 µg/mL), and PNP (20 nm (negatively and positively charged) and 100 nm (negatively charged), 176 µg/mL) on Rt of RAECM after 2, 4 and 24 hours of exposure (n = 5–9 for each condition). Rt of all monolayers prior to apical exposure to nanoparticles (at t = 0) was $2.13 \pm 0.27 \text{ K}\Omega\cdot\text{cm}^2$ (n = 66). * = significantly different (p < 0.05) from control (unexposed monolayers).

Table 1

Chemical composition of UAPS

Chemical species	% by mass
Nitrate	8.76
Sulfate	8.84
Elemental carbon	5.73
Organic carbon	47.80
Trace elements and metals*	15.88
Unknown	13.01

* Predominant components of trace elements and metals were silicon, aluminum, iron, calcium and zinc.

Table 2

Apparent permeability (Papp) of mannitol and inulin

	Control	UAPS
¹⁴ C-Mannitol	7.4 ± 4.2	8.8 ± 8.1
¹⁴ C-Inulin	3.0 ± 2.0	7.0 ± 3.4

Effects of apical exposure to UAPS (36 µg/mL) on apparent permeability coefficient (Papp × 10⁷ cm/s) of RAECM to ¹⁴C-mannitol and ¹⁴C-inulin. Papp are shown as mean ± SEM (n = 3). No significant differences due to UAPS exposure were seen.